Applied Catalysis B: Environmental 144 (2014) 129–134

Contents lists available at ScienceDirect

Applied Catalysis B: Environmental

journal homepage: www.elsevier.com/locate/apcatb

High selectivity of ethanol electrooxidation to carbon dioxide on platinum nanoparticles in low temperature polymer electrolyte membrane direct ethanol fuel cell

Jakub Seweryn, Adam Lewera*

Department of Chemistry, University of Warsaw, ul. Pasteura 1, 02-093 Warsaw, Poland

ARTICLE INFO

Article history:
Received 10 May 2013
Received in revised form 25 June 2013
Accepted 1 July 2013
Available online 11 July 2013

Keywords:
Platinum
Ethanol electrooxidation
Oxygen permeation
Direct ethanol fuel cell

ABSTRACT

Products of ethanol oxidation on Pt/C nanoparticles in low temperature, polymer electrolyte membrane direct ethanol fuel cell are determined qualitatively and quantitatively in broad range of cell voltages and temperatures. Despite the fact that platinum is one of the most popular anode systems studied, comparable literature data are severely limited due to the broad unawareness of the oxygen permeation process occurring in fuel cells. Correction for oxygen crossover from cathode compartment allowed us also to correlate our results to general mechanism of ethanol electrooxidation, determined based on ex situ spectroscopic analysis, as available in literature. We also determined that for certain conditions on platinum anode, in low temperature polymer–electrolyte membrane direct ethanol fuel cell, ethanol is oxidized to carbon dioxide with very high (ca. 82%) selectivity. Conditions required for obtaining the reported selectivity are presented and discussed.

1. Introduction

Process of electrocatalytical oxidation of ethanol on platinum and platinum-group metals has long attracted the attention of many research groups [1–17]. Several approaches have been used to understand the mechanism of electrocatalytical oxidation of ethanol, using broad array of methods, such as IR [6,7,8,15], Raman [18,19] and sum-frequency generation spectroscopy [20–23], mass spectrometry [4,7,13,15] or radiometric [17,22] usually with control of electrode potential. Also in situ tests in working direct ethanol fuel cells (DEFC) were performed [24–31]. Still, the results obtained in fuel cell tests are to some point contrary in regards to distribution of products of ethanol oxidation.

It is generally accepted, that for complete oxidation of ethanol, adsorbed OH groups are needed [1], although they cannot be formed on Pt surface at low electrode potentials to the extend sufficient for creating the significant amount of acetic acid and carbon dioxide. Consequently at low electrode potential virtually no acetic acid (or adsorbed acetyl groups) was found using spectroelectrochemical methods [8,23].

But in case of DEFC experiments with platinum anode there are numerous observations of presence of acetic acid in anode outlet stream, which is contrary to the published ex situ data [8,23]. We have previously provided evidence that this discrepancy can be attributed to chemical oxidation of ethanol by oxygen permeating from cathode side [32,33]. Those preliminary results were focused on oxygen permeation process thus were limited to three distinct temperatures and cell voltage equal or higher than 300 mV. To the best of our knowledge to this time only Nakagawa et al. have presented oxygen-permeation corrected distribution of products of ethanol electrooxidation for Pt/C, PtRu/C and PtRuRh/C DEFC anodes, but limited to 80 °C and cell voltages lower than 200 mV [34]. Here we show a much broader range of both, cell voltage and temperature, covering the common conditions of working DEFC, and limited only by the intrinsic properties of the system studied, which allowed us to comment on distribution of products of ethanol electrooxidation on platinum in working DEFC.

We have also determined the conditions required to oxidize ethanol in DEFC mainly to carbon dioxide, which is an important factor for improvement of efficiency of DEFC. Carbon dioxide is a product of total, 12-electrons oxidation of ethanol, and selective oxidation to carbon dioxide is a prerequisite for construction of highly-effective direct ethanol fuel cell.

2. Experimental

All chemicals were of analytical grade and were used without further purification. MilliQ (18 MΩ cm) water was used in preparation of electrolytes for electrochemical experiments and ethanol

* Corresponding author. Tel.: +48 22 822 0211x524; fax: +48 22 822 0211x524.
E-mail address: alewera@chem.uw.edu.pl (A. Lewera).

0926-3373/$ – see front matter © 2013 Elsevier B.V. All rights reserved.
http://dx.doi.org/10.1016/j.apcatb.2013.07.012

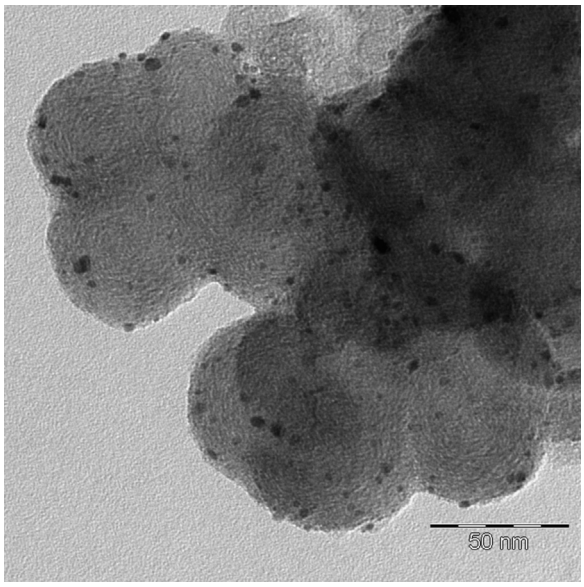

Fig. 1. TEM image of Pt/C catalysts prepared using impregnation–reduction method. Average particle size: 4 nm, metal loading: ca. 18 wt.%.

solution. High purity (N5.2) gases from Air Products were used to deaerate ethanol solutions (Ar) and as a cathode gas (O_2).

2.1. Catalyst preparation and morphology analysis

Pt/C catalyst has been prepared using impregnation–reduction method; detailed description can be found elsewhere [35]. In short, after treatment in aqua regia carbon sample has been mixed with H_2PtCl_6 solution to obtain desired metal loading and reduced in flow of hydrogen/argon mixture at 150 °C. Metal content was ca. 18% by weight. This procedure resulted in uniformly distributed Pt nanoparticles (size ca. 4 nm) on carbon substrate (Fig. 1). Transmission electron microscopy (TEM) imaging was performed using TEM Libra 120 (Zeiss).

2.2. Electrochemical investigation

For electrochemical experiments 10 μl of Pt/C catalyst's suspension in mixture of ethanol, water and Nafion® was placed on gold disk (diameter 3.6 mm), left to dry and used as a working electrode [35]. Catalyst's suspension used consisted of 4.5 mg of catalyst, 280 μl of water, 200 μl of ethanol and 20 μl of 5% Nafion solution in ethanol. Mass of dried deposit was about 120 μg. Cyclic voltammetry experiments were performed in aqueous solutions of: (a) sulfuric acid (0.5 mol dm^{-3}) and (b) ethanol in sulfuric acid, (both 0.5 mol dm^{-3}). All electrode potentials were registered versus Hg/Hg_2SO_4/0.5 M H_2SO_4 reference electrode and later recalculated versus RHE. PINE Instrument AFRDE5 bipotentiostat was used with National Instruments NI DAQ 6211 data acquisition card. Voltammograms have been normalized using the charge associated with hydrogen adsorption, assuming the charge of 210 μC cm^{-2}.

2.3. Fuel cell experiments

For fuel cell experiments, Nafion® 117 membrane was painted in the center with prepared catalysts' suspension on one side as anode, and 40% Pt/C (BASF/ETEK) on the other side as cathode, to obtain a square (area 10 cm^2). Loading of anode and cathode side was approximately 1 mg(metal) cm^{-2}. When dry, each side was covered with pre-cut carbon paper squares and hot-pressed. Fuel cell hardware from Fuel Cell Technologies INC, consisting of two graphite plates with single serpentine flow pattern (10 cm^2 active area) was used. The flow of oxygen at cathode side was maintained at 15 sccm s^{-1} while fuel (0.2 mol dm^{-3} of ethanol in water) was fed at approximately 1 cm^3 min^{-1} rate. Fuel flow rate used has been pre-optimized to obtain: (i) relatively high concentration of products of ethanol oxidation in anode outlet stream, which increases the precision of determination of acetaldehyde and acetic acid concentration, (ii) to avoid fuel starvation conditions. In general the fuel utilization at this flow rate was not exceeding 10%. Flow rate has been kept stable to allow for assessing the carbon dioxide production rate from charge balance.

Ethanol solution was thoroughly deaerated (purged with Ar gas) before and during introducing it to the fuel cell. Fuel cell was operated at 60, 70, 80 and 90 °C and numerous cell voltages (from OCV to 100 mV, separated by 50 mV). Cell voltage and current were controlled using EG&G Princeton Applied Research 362 Scanning Potentiostat with National Instruments NI DAQ 6009 data acquisition card. More details can be found elsewhere [35].

To avoid misunderstanding, electrode (anode, cathode or working electrode) potential is always referred to as "anode potential", "electrode potential" etc. Fuel cell voltage is always referred to as "cell voltage".

Products of ethanol oxidation were sampled from the port, located directly at the anode outlet, then introduced to Hewlett Packard 5890 Series II Gas Chromatograph (GC) equipped with Flame Ionization (FID) and Mass Selective detectors, which allowed for separation and qualitative and quantitative determination of the components of the mixture leaving fuel cell. GC setup has been calibrated prior to the experiment. The response of FID detector to different concentration of ethanol, acetaldehyde and acetic acid in test samples has been determined and used to minimize the possible errors in quantitative analysis. The overall error of quantitative determination of ethanol, acetaldehyde and acetic acid has been well below 1%. Acetic acid and acetaldehyde formation rate was calculated from gas chromatography results, geometric fuel cell active area and fuel flow rate. Amount of CO_2 has been calculated from charge balance using the registered concentration of acetic acid, acetaldehyde, fuel cell active area and the fuel flow rate, as FID detector is insensitive to carbon dioxide.

Data have been corrected for the amount of acetaldehyde and acetic acid produced due to oxygen permeation by subtracting the amounts obtained in currentless conditions [32,33,35]. The contribution of oxygen permeation to the total amounts of products observed changes from 100% at OCV, ca. 20% at 300 mV and ca. 10% at 100 mV. It is worth to note that the ethanol oxidation products observed in currentless conditions are formed as a result of catalytic oxidation of ethanol by the oxygen permeating from the cathode side. Thus the observed amounts of products in currentless conditions are estimates of the lowest possible rate of oxygen permeation.

3. Results and discussion

3.1. Electrochemical investigation

Voltammetric responses of Pt/C catalyst deposited on gold substrate were registered in supporting electrolyte (0.5 mol dm^{-3} sulfuric acid) and in 0.5 mol dm^{-3} ethanol in 0.5 mol dm^{-3} sulfuric acid (Fig. 2A and B, respectively). The registered response is typical for metallic platinum: hydrogen adsorption/desorption signals at electrode potentials lower than 200 mV and Pt oxide formation (anodic scan, $E > 700$ mV) and their reduction (cathodic scan, E ca. 700 mV) are observed (Fig. 2A).

Voltammogram registered in H_2SO_4/ethanol solution (Fig. 2B) is typical for ethanol electrooxidation on platinum at those conditions

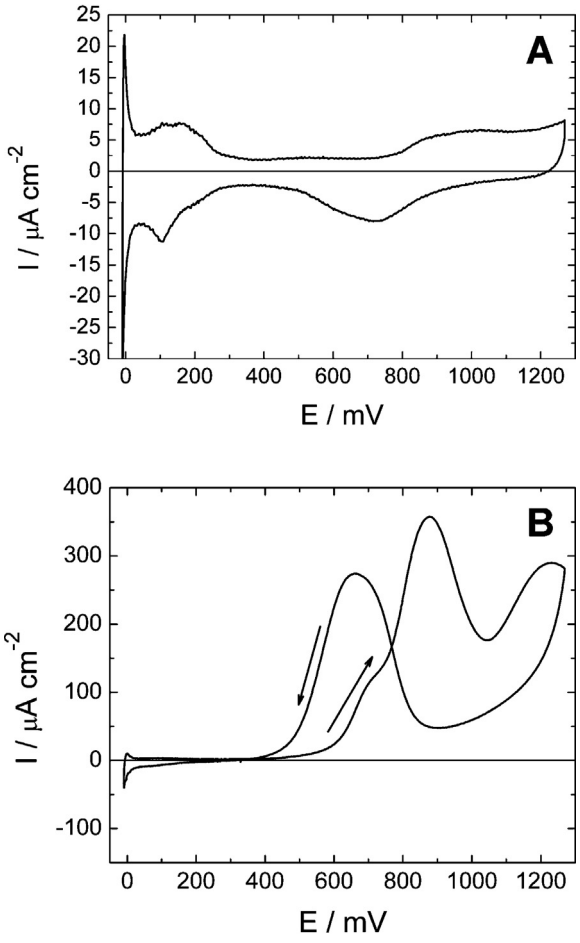

Fig. 2. Voltamperometric response of Pt/C catalyst synthesized using impregnation–reduction method. Experiment performed in 0.5 mol dm^{-3} H_2SO_4 (A) and 0.5 mol dm^{-3} H_2SO_4 and 0.5 mol dm^{-3} ethanol (B).

and confirms high activity of material obtained [1]. Observable currents in anode scan starts at ca. 400 mV and are reaching first maximum at ca. 880 mV. Then the current decrease, reaching minimum at ca. 1050 mV to rise again and reach second maximum at 1180 mV. In the cathodic scan one maximum is observed at ca. 650 mV, and the voltammogram forms a typical shape with observable hysteresis. Additionally on the first oxidation peak a small peak can be observed at ca. 700 mV. The above mentioned features can be attributed to the complex mechanism of ethanol electrooxidation, where at low electrode potentials ethanol adsorbs dissociatively on Pt surface, resulting in surface blocked by adsorbed carbon monoxide [36]. When electrode potential increases, CO is oxidized and ethanol can be electrooxidized, which is responsible for formation of two above mentioned peaks (at 880 and 1180 mV) [1]. The small peak at ca. 700 mV is caused by oxidation of ethanol on Pt(1 0 0) plane in presence of sulfate ions [37], and the decrease of current at ca. 1050 mV is caused by concurrent adsorption of water or anions – most probably (bi)sulfates [38–40].

It is well established, that depending on the electrode potential, different mechanisms of ethanol electrooxidation can be observed: up to ca. 600 mV ethanol can be electrooxidized to acetaldehyde, which is a product of simple dehydrogenation of ethanol molecule. In this process two electrons are released. Electrooxidation of ethanol to acetic acid (4-electrons process) or carbon dioxide (12-electrons) requires a source of additional oxygen atoms, which usually come from adsorbed OH groups. Those groups cannot be formed in large quantities on platinum surface when electrode potential is lower than 500 mV vs. RHE [8,21,23]. Additionally it has been presented, that in the presence of ethanol, the adsorbed OH groups cannot be formed in detectable amounts as long as surface is covered with adsorbed carbon monoxide [8,23]. Onset of carbon monoxide oxidation is observed at ca. 400 mV, and at 600–700 mV this process is fast enough to completely remove adsorbed CO from Pt surface. This is most probably the cause why acetic acid can be detected using spectroscopy methods only at electrode potentials above 600 mV [8,23]. Formation of adsorbed OH groups and subsequent oxidation or ethanol to acetic acid and carbon dioxide explains also the observed increase in voltammetric current, when electrode potential is higher than 600 mV (Fig. 2B).

Additionally a direct mechanism of electrooxidation of ethanol to CO_2 has been proposed for low electrode potentials (400–600 mV), based on assumption of dissociative adsorption of ethanol on Pt surface, but the source of additional oxygen atom required for such reaction is unclear, especially at the electrode potentials lower than 500 mV [12,41].

3.2. Fuel cell experiments

Fig. 3 shows the production rate of acetaldehyde (A), acetic acid (B) and carbon dioxide (C). Production rate of acetaldehyde and acetic acid was calculated based on registered concentration of respective compounds in fuel cell outlet stream in numerous cell conditions (temperature, cell voltage – see Section 2), fuel flow rate and geometric fuel cell active area. Carbon dioxide production rate was calculated from products' concentration registered in anode outlet stream and registered current flow to balance the charge (see Section 2). Upper cell voltage limit of the determined production rate is limited by OCV values at respective conditions. The registered open circuit voltages were as follows: 500 mV; 535 mV; 545 mV and 560 mV for 60 °C; 70 °C; 80 °C and 90 °C respectively.

In the broad cell voltage and temperature ranges it can be observed, that acetaldehyde is already produced at relatively high cell voltage (ca. 400 mV), and the amount of acetaldehyde produced is dependent almost exclusively on cell voltage (Fig. 3A). Overall the acetaldehyde production is relatively small, reaching 9 nmol cm^{-2} s^{-1} at cell voltage close to 100 mV and temperature equal to 90 °C. The decrease of temperature to 60 °C and keeping cell voltage constant at 100 mV only slightly decrease the amount of acetaldehyde produced, to ca. 8 nmol cm^{-2} s^{-1} (Fig. 3A).

Acetic acid is detected at cell voltage equal or lower than 300 mV. It has been already shown by us, that acetic acid production on platinum catalyst in fuel cell is close to zero, when cell voltage is 300 mV or more [33]. But its production rate grows quickly as cell voltage is decreased below 300 mV. This is overall in agreement with ethanol oxidation mechanism, as discussed above. Additionally amount of acetic acid increases when cell temperature increases. It reaches ca. 27 nmol cm^{-2} s^{-1} at cell voltage equal to 100 mV and temperature 90 °C. It decreases to half of that value when temperature decreases to 60 °C, still at cell voltage equal to 100 mV (Fig. 3B).

Carbon dioxide production is highly dependent on both: cell voltage and temperature. In general onset of its production occurs earlier than onset of acetic acid production, especially at elevated temperatures (Fig. 3B and C). Amount of carbon dioxide produced reaches 54 nmol cm^{-2} s^{-1} at cell voltage ca. 100 mV and temperature 90 °C. Its amount decreases 4-fold when temperature was decreased to 60 °C (Fig. 3C).

Connecting electrochemical results with fuel cell data leads to the following conclusions: when anode potential is lower than 500 mV, no significant amounts of acetic acid or carbon dioxide should be formed as a result of electrode reaction. Assuming that cathode potential equal ca. 800 mV (the potential of oxygen reduction on platinum) then anode potential equal to 500 mV represents ca. 300 mV of cell voltage. Concluding, based on the literature data discussed above, in the conditions when cell voltage is higher than

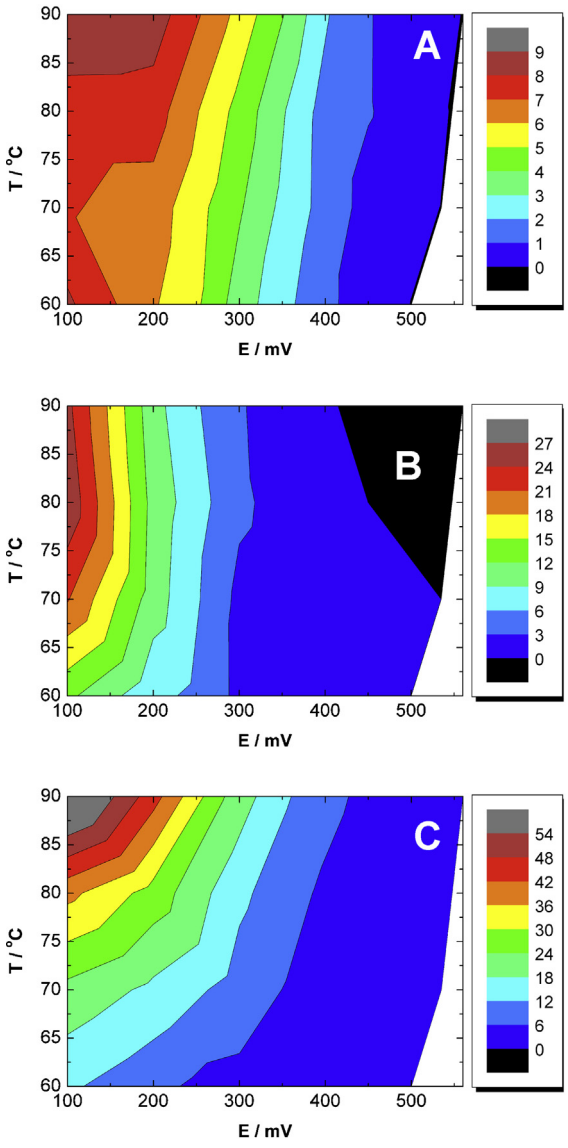

Fig. 3. Oxygen-permeation corrected amounts of acetaldehyde (A), acetic acid (B) and carbon dioxide (calculated) (C) produced at Pt anode in nmol cm^{-2} s^{-1} in working low temperature fuel cell as a function of cell voltage and temperature. Please note, that color scale varies between each graph to emphasize temperature and cell voltage dependence. (For interpretation of the references to color in this figure legend, the reader is referred to the web version of the article.)

approximately 300 mV, there should be no significant amounts of acetic acid or carbon dioxide detected, which is in agreement with our results. But there are numerous reports where significant amounts of acetic acid have been found at the anode outlet of working fuel cell, when Pt has been used as anode catalysts, i.e. [25,26]. Obviously, based on the mechanism of electrooxidation of ethanol on platinum surface, acetic acid cannot be formed as a result of electrode reaction in those conditions [1]. In fact it has been previously shown by us [32,33], that the observed acetic acid is the product of chemical oxidation of ethanol by the oxygen permeating from cathode side, which explains the contradiction between the broadly accepted mechanism of ethanol electrooxidation on platinum determined based on ex situ measurements (electrochemical, spectroelectrochemical) and observation of acetic acid at low anode potentials.

Except preliminary data reported by us [32,33] in the literature there is only one report of distribution of products of ethanol electrooxidation when oxygen permeation has been corrected for [34]. That report is focused on ethanol electrooxidation on Pt/C, PtRu/C and PtRuRh/C nanoparticles at 80 °C and cell voltage below 200 mV. When comparing our (Fig. 3) and the reported in [34] acetaldehyde and acetic acid amounts produced in the process of ethanol (0.5 mol dm^{-3}) electrooxidation on Pt/C catalyst it can be found, that our results are similar qualitatively but 2–3 times higher quantitatively (Fig. 3) in the corresponding conditions. In case of carbon dioxide our results indicate even higher difference (up to 15 times). The most probable explanation of the observed disagreement is that in [34] authors collected the products from the FC anode for 2 h before analysis. This approach may lead to significant loss of dissolved CO_2 and overall to underestimation of its content, especially because fuel cell was operated at relatively high temperature (80 °C). To some extent the difference between reported and measured values can be also the result of different anode catalyst loading (about 2.7 mg cm^{-2} [34] whereas we used approximately 1 mg cm^{-2}), different membrane, or difference in ethanol concentration used.

Registered amounts of products of ethanol electrooxidation in wide range of cell conditions (see Section 2) can be recalculated to determine the molar percentage of each products observed at outlet stream (Fig. 4). Due to the low overall amounts, the magnitude of experimental error is higher at high cell voltages. This most probably explains the "island" present at Fig. 4B (E = 450 mV, T = 70 °C). The following general trends can be observed: acetaldehyde production dominates at relatively low temperature (60 °C) and cell voltage close to 300 mV (Fig. 4A). Obviously this is due to the fact, that at those conditions neither acetic acid nor carbon dioxide is formed in significant amounts. Acetic acid production is highest at low cell voltage (lower than 200 mV) and moderate temperature (60–80 °C). Carbon dioxide production dominates at high temperature (80 °C and more) and cell voltage close to 400 mV.

To the extent, where our data regarding product distribution can be compared to the above mentioned literature [34], quite good agreement has been observed. In particular, for cell voltage in range between 200 and 100 mV and temperature equal to 80 °C reported selectivity toward acetaldehyde decreased from ca. 30% to 12%, selectivity toward acetic acid increased from ca. 45% to 55% and selectivity toward carbon dioxide increased from ca. 27% to 32%[34]. The trends observed by us were identical (Fig. 4). However it must be remembered, that our data is based on absolute values of production rate/concentration in outlet stream, whereas in [34] the reported values are selectivities, which means that results in [34] were recalculated to determine how many ethanol molecules are oxidized to either acetaldehyde, acetic acid and carbon dioxide molecules, using Eq. (4) in [34]. It is unclear why authors in [34] multiplied the amount of carbon dioxide by two instead of dividing it by two, to calculate the selectivity toward CO_2, nevertheless in general, as compared to our results, selectivity data obtained based on Eq. (4) in [34] will show increased amount of carbon dioxide (by a factor of four) and decreased amounts of acetic acid and acetaldehyde (to the extent dependent on carbon dioxide amounts). In addition, the probable loss of carbon dioxide, as discussed above, additionally change the balance, this time decreasing the selectivity toward CO_2 and to some extend canceling the effect of multiplication of CO_2 amount (Eq. (4) in [34]).

Regarding the product distribution data obtained by us, in comparable conditions as in [34], we observed that amount of acetaldehyde decreased from 22% to 13%, amount of acetic acid increased from 26 to 37% and amount of carbon dioxide was almost constant at 62%. Based on the discussion of possible differences (see above), we can conclude, that out data are quite consistent with those presented in [34], but probably more precise.

The observation that highest relative amount of carbon dioxide can be found at cell voltage close to 400 mV requires further analysis. It is worth noting that Rao et al. using gas diffusion electrode

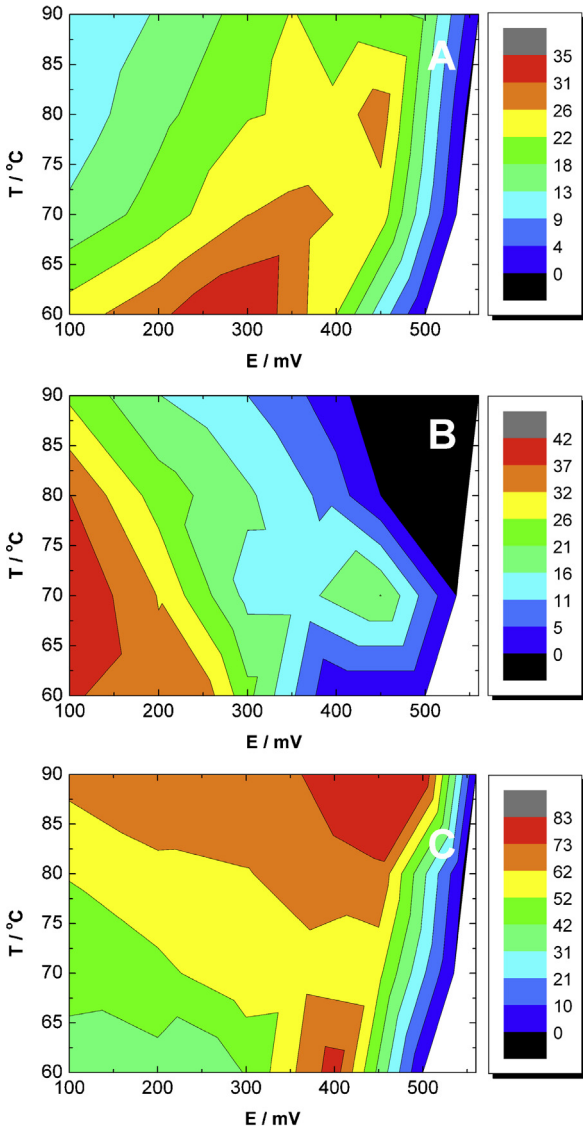

Fig. 4. Oxygen-permeation corrected molar percents of acetaldehyde (A), acetic acid (B) and carbon dioxide (calculated) (C) produced at Pt anode in working low temperature fuel cell as a function of cell voltage and temperature. Please note, that color scale varies between each graph to emphasize temperature and cell voltage dependence. (For interpretation of the references to color in this figure legend, the reader is referred to the web version of the article.)

experiments found, that in ethanol oxidation on Pt, CO_2 current efficiency has maximum in the 500–600 mV range, reaching 75%, and decreases when electrode potential increase [42] (which correspond to decrease of cell voltage), which supports our observation of 82% maximum at similar anode potential and further decrease (Fig. 4C). The difference is caused by the fact, that "current efficienc" used in [42] does not equal to "relative amounts" as used here. Current efficiency value for every product is equal to relative amount of that product, weighted by respective number of electrons released, i.e. 6 for CO_2, 4 for acetic acid and 2 for acetaldehyde (see Eqs. (1)–(2) in [42]). In general both values converge at their respective maximum values. This additionally supports our results in comparison to above mentioned results presented in [34].

Regardless of the exact value of amount of carbon dioxide produced, its source at those electrode potentials is not well established. It has been suggested, that CO_2 can be the result of dissociative adsorption of ethanol, which can occur when electrode potential is relatively low (from 100 mV to the onset of CO oxidation), which results in electrode surface covered by adsorbed CO [12,41], but the source of additional oxygen atom, required to oxidize adsorbed CO to CO_2 is unclear. The most probable explanation is that at those electrode potentials a small amount of adsorbed OH groups are already present. Observation of carbon dioxide in those conditions is consistent also with conclusion derived in [10,12,23], that around the 400–500 mV the oxidation of adsorbed CO species (most probably resulting from ethanol dissociative adsorption) begins, leading to the formation of CO_2. Obviously the absolute amounts of carbon dioxide produced at that electrode potential are small (Fig. 3C). This observation suggests, that in those conditions oxidation of ethanol to carbon dioxide (albeit slow) is preferred, as oxidation to acetic acid seems to require more positive electrode potential (Fig. 4B). Obviously in this region adsorbed OH groups (or just formed OH groups) seems to be used exclusively and totally in the process of oxidation of ethanol to CO_2, not to acetic acid. This may also explain why adsorbed OH groups are not observed at that electrode potential range [8,23]. This subject as still unclear requires further studies.

4. Conclusions

Our results show that correction for oxygen permeation is required to obtain good relationship between data related to ethanol electrooxidation products' distribution obtained in fuel cell experiments and those obtained in ex situ experiments. It has been shown, that until cell voltage drops below 300 mV then acetic acid cannot be formed in significant amounts as a result of ethanol electrooxidation. In those condition the main product is acetaldehyde and – to varied extend – carbon dioxide (Figs. 3 and 4).

Furthermore, below cell voltage 300 mV the acetic acid production increased, most probably due to the liberating of platinum surface via oxidation of adsorbed CO species and oxidation of water to produce adsorbed OH groups. This is clearly visible in Fig. 3B showing rapid increment of acid production above the 250 mV and can be connected to the shape of voltammogram registered in presence of ethanol (Fig. 2B). As the acetic acid is effective a dead-end of ethanol oxidation in low temperature fuel cells, those conditions should be avoided.

The region of relative dominance (up to 82%) of complete oxidation of ethanol to carbon dioxide has been determined to be centered at cell voltage of approximately 400 mV that coincides with onset of adsorbed CO oxidation. This cell voltage is too high for acetic acid production. Despite relatively low current density in those conditions, determination of the conditions where oxidation of ethanol to carbon dioxide dominates, as well as undisturbed distribution of products of ethanol electrooxidation on platinum can help to further advance the fuel cell research. This emphasizes the importance of analysis of products and by-products of ethanol electrooxidation.

Acknowledgements

This work has been financially supported by Ministry of Science and Higher Education (Poland) under the grant N N204 527739. We thank Aneta Januszewska and Marianna Gniadek for performing TEM imaging. The TEM images were obtained using the equipment purchased within CePT Project No.: POIG.02.02.00-14-024/08-00.

References

[1] H. Hitmi, E.M. Belgsir, J.M. Leger, C. Lamy, R.O. Lezna, Electrochimica Acta 39 (1994) 407–415.
[2] B. Bittins-Cattaneo, S. Wilhelm, E. Cattaneo, H.W. Buschmann, W. Vielstich, Physical Chemistry Chemical Physics 92 (1988) 1210–1218.
[3] T. Iwasita, R. Dalbeck, E. Pastor, X. Xia, Electrochimica Acta 39 (1994) 1817–1823.

[4] J.T. Wang, S. Wasmus, R.F. Savinell, Journal of the Electrochemical Society 142 (1995) 4218–4224.
[5] E. Antolini, Journal of Power Sources 170 (2007) 1–12.
[6] F. Vigier, C. Coutanceau, F. Hahn, E.M. Belgsir, C. Lamy, Journal of Electroanalytical Chemistry 563 (2004) 81–89.
[7] J.P.I. de Souza, S.L. Queiroz, K. Bergamaski, E.R. Gonzalez, F.C. Nart, Journal of Physical Chemistry B 106 (2002) 9825–9830.
[8] M. Heinen, Z. Jusys, R.J. Behm, Journal of Physical Chemistry C 114 (2010) 9850–9864.
[9] C. Lamy, E.M. Belgsir, J.M. Leger, Journal of Applied Electrochemistry 31 (2001) 799–809.
[10] J.M. Leger, S. Rousseau, C. Coutanceau, F. Hahn, C. Lamy, Electrochimica Acta 50 (2005) 5118–5125.
[11] F. Vigier, S. Rousseau, C. Coutanceau, J.M. Leger, C. Lamy, Topics in Catalysis 40 (2006) 111–121.
[12] H. Wang, Z. Jusys, R.J. Behm, Journal of Physical Chemistry B 108 (2004) 19413–19424.
[13] H. Wang, Z. Jusys, R.J. Behm, Journal of Power Sources 154 (2006) 351–359.
[14] C. Bianchini, P.K. Shen, Chemical Reviews 109 (2009) 4183–4206.
[15] T. Iwasita, E. Pastor, Electrochimica Acta 39 (1994) 531–537.
[16] S.C.S. Lai, M.T.M. Koper, Faraday Discussions 140 (2008) 399–416.
[17] E. Pastor, T. Iwasita, Electrochimica Acta 39 (1994) 547–551.
[18] S.C.S. Lai, S.E.F. Kleyn, V. Rosca, M.T.M. Koper, Journal of Physical Chemistry C 112 (2008) 19080–19087.
[19] S.C.S. Lai, M.T.M. Koper, Physical Chemistry Chemical Physics 11 (2009) 10446–10456.
[20] A. Wieckowski, R.B. Kutz, B. Braunschweig, P. Mukherjee, R.L. Behrens, D.D. Dlott, Journal of Catalysis 278 (2011) 181–188.
[21] B. Braunschweig, P. Mukherjee, R.B. Kutz, A. Wieckowski, D.D. Dlott, Journal of Chemical Physics 133 (2010) 234702.
[22] R.B. Kutz, B. Braunschweig, P. Mukherjee, D.D. Dlott, A. Wieckowski, Journal of Physical Chemistry Letters 2 (2011) 2236–2240.
[23] R.B. Kutz, B. Braunschweig, P. Mukherjee, R.L. Behrens, D.D. Dlott, A. Wieckowski, Journal of Catalysis 278 (2011) 181–188.
[24] G. Andreadis, V. Stergiopoulos, S. Song, P. Tsiakaras, Applied Catalysis B 100 (2010) 157–164.
[25] D.D. James, D.V. Bennett, G.C. Li, A. Ghumman, R.J. Helleur, P.G. Pickup, Electrochemistry Communications 11 (2009) 1877–1880.
[26] S. Rousseau, C. Coutanceau, C. Lamy, J.M. Leger, Journal of Power Sources 158 (2006) 18–24.
[27] S.Q. Song, W.J. Zhou, Z.H. Zhou, L.H. Jiang, G.Q. Sun, Q. Xin, V. Leontidis, S. Kontou, P. Tsiakaras, International Journal of Hydrogen Energy 30 (2005) 995–1001.
[28] W.J. Zhou, B. Zhou, W.Z. Li, Z.H. Zhou, S.Q. Song, G.Q. Sun, Q. Xin, S. Douvartzides, A. Goula, P. Tsiakaras, Journal of Power Sources 126 (2004) 16–22.
[29] W.J. Zhou, Z.H. Zhou, S.Q. Song, W.Z. Li, G.Q. Sun, P. Tsiakaras, Q. Xin, Applied Catalysis B 46 (2003) 273–285.
[30] A. Brouzgou, A. Podias, P. Tsiakaras, Journal of Applied Electrochemistry 43 (2013) 119–136.
[31] A. Brouzgou, S.Q. Song, P. Tsiakaras, Applied Catalysis B 127 (2012) 371–388.
[32] A. Jablonski, P.J. Kulesza, A. Lewera, Journal of Power Sources 196 (2011) 4714–4718.
[33] A. Jablonski, A. Lewera, Applied Catalysis B 115 (2012) 25–30.
[34] N. Nakagawa, Y. Kaneda, M. Wagatsuma, T. Tsujiguchi, Journal of Power Sources 199 (2012) 103–109.
[35] J. Seweryn, A. Lewera, Journal of Power Sources 205 (2012) 264–271.
[36] J. Souza-Garcia, E. Herrero, J.M. Feliu, Chemphyschem 11 (2010) 1391–1394.
[37] C. Buso-Rogero, V. Grozovski, F.J. Vidal-Iglesias, J. Solla-Gullon, E. Herrero, J.M. Feliu, Journal of Materials Chemistry A 1 (2013) 7068–7076.
[38] X.H. Xia, H.D. Liess, T. Iwasita, Journal of Electroanalytical Chemistry 437 (1997) 233–240.
[39] M.E. Gamboaaldeco, E. Herrero, P.S. Zelenay, A. Wieckowski, Journal of Electroanalytical Chemistry 348 (1993) 451–457.
[40] E. Herrero, K. Franaszczuk, A. Wieckowski, Journal of Electroanalytical Chemistry 361 (1993) 269–273.
[41] R. Ianniello, V.M. Schmidt, J.L. Rodriguez, E. Pastor, Journal of Electroanalytical Chemistry 471 (1999) 167–179.
[42] V. Rao, C. Cremers, U. Stimming, L. Cao, S.G. Sun, S.Y. Yan, G.Q. Sun, Q. Xin, Journal of the Electrochemical Society 154 (2007) B1138–B1147.